

**\*\*TITLE\*\***

*ASP Conference Series, Vol. \*\*VOLUME\*\*, \*\*YEAR OF PUBLICATION\*\**

**\*\*NAMES OF EDITORS\*\***

## The Iron Project and Non-LTE stellar modeling

Sultana N. Nahar

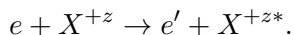
*Dept of Astronomy, Ohio State University, Columbus, OH 43210, USA*

**Abstract.** Latest developments in theoretical computations since the international Opacity Project (OP), under the new the Iron Project (IP) and extensions, are described for applications to a variety of objects such as stellar atmospheres, nebulae, and active galactic nuclei. The primary atomic processes are: electron impact excitation (EIE), photoionization, electron-ion recombination, and bound-bound transitions, all considered using the accurate and powerful R-matrix method including relativistic effects. As an extension of the OP and the IP, a self-consistent and unified theoretical treatment of photoionization and recombination has been developed. Both the radiative and the dielectronic recombination (RR and DR) processes are considered in a unified manner. Photoionization and recombination cross sections are computed with identical wavefunction expansions, thus ensuring self-consistency in an ab initio manner. The new unified results differ from the sum of previous results for RR and DR by up to a factor of 4 for the important but complex atomic systems such as Fe I - V. The fundamental differences are due to quantum mechanical interference and coupling effects neglected in simpler approximations that unphysically treat RR and DR separately, which can not be independently measured or observed. The electronic, web-interactive, database, TIPTOPBASE, to archive the OP/IP data in a readily accessible manner is also described. TIPTOPBASE would include electron-ion recombination data and new fine structure transition probabilities. Efficient codes developed by M.J. Seaton to calculate ‘customized’ mixture opacities and radiative accelerations (‘levitation’) in stars will also be available.

### 1. Introduction

At densities and temperatures in stellar atmospheres, many atomic levels are excited under non-local thermal equilibrium (NLTE) conditions. NLTE models and other applications such as stellar opacities require large amount of accurate atomic parameters for collisional and radiative processes to describe radiation transfer, spectral analysis etc. The collisional process is primarily electron impact excitation (EIE), while radiative processes are photoionization, electron-ion recombination, and bound-bound transitions. These four basic dominant atomic processes in the plasmas can be described as follows.

i) Electron-impact excitation (EIE) of an ion  $X^{+z}$  of charge  $z$ :



ii) Radiative bound-bound transitions:

$$X^{+z} + h\nu \rightleftharpoons X^{+z*},$$

iii) Photoionization (PI) by absorption of a photon:

$$X^{+z} + h\nu \rightleftharpoons X^{+z+1} + \epsilon.$$

The inverse process of PI is electron-ion radiative recombination (RR).

iv) Autoionization (AI) and dielectronic recombination (DR):

$$e + X^{+z} \rightarrow (X^{+z-1})^{**} \rightarrow \begin{cases} e + X^{+z} & \text{AI} \\ X^{+z-1} + h\nu & \text{DR} \end{cases}$$

The inverse process of DR is photoionization via the intermediate doubly excited autoionizing states, i.e. resonances in atomic processes. At prevailing densities and temperatures in stellar atmospheres, the role of metastable states and low-lying fine structure levels in photoionization and recombination of ions bears special emphasis.

Collisional and radiative atomic process have been studied in ab initio manner under the OP (*The Opacity Project* 1995, 1996), and the IP (Hummer et al. 1993). The close coupling R-matrix methodology employed under the OP and IP enables the computation of self-consistent sets of atomic parameters, thereby reducing uncertainties in applications involving different processes and approximations. Sample results obtained under the two projects are presented.

## 2. Theory

Atomic processes are treated in an ab initio manner in the close coupling (CC) approximation employing the R-matrix method (e.g. Burke & Robb 1975, Seaton 1987, Berrington et al. 1987, Berrington et al. 1995). The total wavefunction for a (N+1) electron system in the CC approximation is described as:

$$\Psi_E(e + ion) = A \sum_i^N \chi_i(ion) \theta_i + \sum_j c_j \Phi_j(e + ion), \quad (1)$$

where in the first term  $\chi_i$  is the target ion or core wavefunction in a specific state  $S_i L_i \pi_i$  or level  $J_i \pi_i$ ,  $\theta_i$  is the wavefunction of the interacting (N+1)th electron in a channel labeled as  $S_i L_i (J_i) \pi_i k_i^2 \ell_i (SL\pi \text{ or } J\pi)$ ,  $k_i^2$  is the incident kinetic energy. In the second term,  $\Phi_j$  is the correlation functions of (e+ion) system that compensates the orthogonality condition and short range correlation interactions. The complex resonant structures in photoionization, recombination, and in electron impact excitation are included through channel couplings. The target wavefunctions are obtained from configuration interaction atomic structure calculations using code, such as, SUPERSTRUCTURE (Eissner et al. 1974).

The relativistic (N+1)-electron Hamiltonian for the N-electron target ion and a free electron in the Breit-Pauli approximation, as adopted under the IP, is

$$H_{N+1}^{\text{BP}} = H_{N+1}^{\text{NR}} + H_{N+1}^{\text{mass}} + H_{N+1}^{\text{Dar}} + H_{N+1}^{\text{so}}, \quad (2)$$

where non-relativistic Hamiltonian is

$$H_{N+1}^{NR} = \sum_{i=1}^{N+1} \left\{ -\nabla_i^2 - \frac{2Z}{r_i} + \sum_{j>i}^{N+1} \frac{2}{r_{ij}} \right\}. \quad (3)$$

The mass correction, Darwin, and spin-orbit interaction terms are:

$$H_{N+1}^{\text{mass}} = -\frac{\alpha^2}{4} \sum_i p_i^4, \quad H_{N+1}^{\text{Dar}} = \frac{Z\alpha^2}{4} \sum_i \nabla^2 \left( \frac{1}{r_i} \right), \quad H_{N+1}^{\text{so}} = Z\alpha^2 \sum_i \frac{1}{r_i^3} \mathbf{l}_i \cdot \mathbf{s}_i. \quad (4)$$

Spin-orbit interaction splits the LS terms into fine-structure  $J$ -levels.

The set of  $SL\pi$  are recoupled to obtain (e + ion) states with total  $J\pi$ , following the diagonalization of the (N+1)-electron Hamiltonian to solve

$$H_{N+1}^{BP} \Psi_E = E \Psi_E. \quad (5)$$

Substitution of the wavefunction expansion introduces a set of coupled equations that are solved using the R-matrix approach. The continuum wavefunction,  $\Psi_F$ , describe the scattering process with the free electron interacting with the target at positive energies ( $E > 0$ ), while at *negative* total energies ( $E < 0$ ), the solutions correspond to pure bound states  $\Psi_B$ .

## 2.1. Electron Impact Excitation

Electron impact excitation is one of the primary processes for spectral formation in astrophysical and laboratory plasmas. The collision strength for transition by electron impact excitation from the initial state of the target ion  $S_i L_i$  to the final state  $S_j L_j$  is given by

$$\Omega(S_i L_i - S_j L_j) = \frac{1}{2} \sum_{SL\pi} \sum_{l_i l_j} (2S+1)(2L+1) |\mathbf{S}^{SL\pi}(S_i L_i l_i - S_j L_j l_j)|^2, \quad (6)$$

where  $\mathbf{S}$  is the scattering matrix, and  $S, L$  are the spin multiplicity and total orbital angular momentum of the (e,ion) system. The effective collision strength or the Maxwellian averaged collision strength can be obtained as

$$\Upsilon(T) = \int_0^\infty \Omega_{ij}(\epsilon_j) e^{\frac{-\epsilon_j}{kT}} d(\epsilon_j/kT), \quad (7)$$

and the excitation rate coefficient for transtion from level  $i \rightarrow j$  as,  $q_{ij}(T) = (8.63 \times 10^{-6} / g_i T^{1/2}) e^{-E_{ij}/kT} \Upsilon(T)$  in  $\text{cm}^3 \text{s}^{-1}$ , where  $T$  is in K,  $E_{ij} = E_j - E_i$ ,  $E_i < E_j$  are in Rydbergs ( $1/kT = 157885/T$ ), and  $g_i$  is the statistical weight of  $i$ .

## 2.2. Photoionization, Recombination, Transition Probabilities

The transition matrix elements for radiative bound-bound excitation or de-excitation can be obtained using bound-state wavefunctions as  $\langle \Psi_B | \mathbf{D} | \Psi_{B'} \rangle$ , and for photoionization and recombination using the bound and continuum wavefunctions as  $\langle \Psi_B | \mathbf{D} | \Psi_F \rangle$ ;  $\mathbf{D}$  is the dipole operator. In "length" form,

$\mathbf{D}_L = \sum_i r_i$ , and in "velocity" form,  $\mathbf{D}_V = -2 \sum_i \Delta_i$ , where the sum corresponds to number of electrons.

The transition matrix element with the dipole operator can be reduced to the generalized line strength defined, in either length or velocity form, as

$$S_L = | \langle \Psi_j | \mathbf{D}_L | \Psi_i \rangle |^2 = \left| \left\langle \Psi_f \left| \sum_{j=1}^{N+1} r_j \right| \Psi_i \right\rangle \right|^2, \quad (8)$$

$$S_V = E_{ij}^{-2} | \langle \Psi_j | \mathbf{D}_V | \Psi_i \rangle |^2 = \omega^{-2} \left| \left\langle \Psi_f \left| \sum_{j=1}^{N+1} \frac{\partial}{\partial r_j} \right| \Psi_i \right\rangle \right|^2. \quad (9)$$

where  $\omega$  is the incident photon energy in Rydberg units, and  $\Psi_i$  and  $\Psi_f$  are the initial and final state wave functions.

The oscillator strength  $f_{ij}$  and the transition probability  $A_{ji}$  for the bound-bound transition are obtained in atomic units (a.u.) as

$$f_{ij} = \frac{E_{ji}}{3g_i} S, \quad A_{ji}(a.u.) = \frac{1}{2} \alpha^3 \frac{g_i}{g_j} E_{ji}^2 f_{ij}, \quad (10)$$

where  $E_{ji}$  is the transition energy,  $\alpha$  is the fine structure constant, and  $g_i$ ,  $g_j$  are the statistical weights. The lifetime of a level  $j$  decaying to all lower levels  $i$ , is  $\tau_j = (\sum_i A_{ji}(s^{-1}))^{-1}$ ,  $A_{ji}(s^{-1}) = A_{ji}(a.u.)/\tau_0$ ,  $\tau_0 = 2.4191 \times 10^{-17}$  is the atomic unit of time.

The photoionization cross section ( $\sigma_{PI}$ ) is proportional to the generalized line strength ( $S$ ),

$$\sigma_{PI} = \frac{4\pi}{3c} \frac{1}{g_i} \omega S. \quad (11)$$

The unified electron-ion recombination method (Nahar & Pradhan 1994,1995) considers the infinite number of recombined states, and incorporates non-resonant and resonant (radiative and dielectronic) recombinations RR and DR. The recombined states are divided into two groups. The contributions from states with  $n \leq 10$  (group A) are obtained from  $\sigma_{PI}$  using principle of detailed balance, while the contributions from states with  $10 < n \leq \infty$  (group B), which are dominated by narrow dense resonances, are obtained from an extension of the DR theory of Bell & Seaton (1985, Nahar & Pradhan 1994).

The recombination cross section,  $\sigma_{RC}$ , is related to  $\sigma_{PI}$  through the principle of detailed balance,

$$\sigma_{RC} = \sigma_{PI} \frac{g_i}{g_j} \frac{h^2 \omega^2}{4\pi^2 m^2 c^2 v^2}. \quad (12)$$

The recombination rate coefficient,  $\alpha_{RC}$ , is obtained from Maxwellian average over  $\sigma_{RC}$  as

$$\alpha_{RC}(T) = \int_0^\infty v f(v) \sigma_{RC} dv, \quad (13)$$

where  $f(v)$  is the Maxwellian velocity distribution function. However, the total  $\alpha_{RC}$  is obtained from the summed contributions from infinite number of recombined states.

The DR cross sections of the high- $n$  states is,  $\sigma_{DR}(k^2; i, j) = g_i k^2 \Omega_{DR}(k^2; i, j)$ . where the DR collision strength is

$$\Omega(DR) = \sum_{SL\pi} \sum_n (1/2)(2S+1)(2L+1)P_n^{SL\pi}. \quad (14)$$

$P_n^{SL\pi}$  is the DR probability in entrance channel  $n$  (Nahar & Pradhan 1994).

### 2.3. Ionization fractions in plasma equilibrium

The main application of self-consistent sets of atomic data for photoionization and electron-ion recombination is in determining ionization fractions in photoionization or collisional (coronal) equilibrium in astrophysical plasmas. Coronal equilibrium corresponds to the balance between electron impact ionization and the electron-ion recombination

$$N(z-1)S(z-1) = N(z)\alpha_{RC}(z) \quad (15)$$

where  $S(z-1)$  is total electron impact ionization rate coefficient which are in general available from various experiments. Photoionization equilibrium in the presence of dominant radiative source is balance photoionization and electron-ion recombination

$$N(z) \int_{\nu_0}^{\infty} \frac{4\pi J_{\nu}}{h\nu} \sigma_{PI}(z, \nu) d\nu = N_e N(z+1) \alpha_{RC}(z, T_e), \quad (16)$$

where  $J_{\nu}$  is photoionizing radiation flux,  $\nu_0$  is ionization potential of the ion, and  $\sigma_{PI}$  refers to photoionization cross sections. Use of self-consistent data for  $\sigma_{PI}$  on the left-hand-side, and  $\alpha_{RC}$  on the right-hand-side, should yield accurate ionization balance.

## 3. Results from the Iron Project

The collisional strengths and most of the radiative data are reported in the "Atomic data from the IRON Project" series in Astronomy and Astrophysics journal (and in its previous Supplements).

Sample results are discussed for each atomic process below: Maxwellian averaged excitation collision strengths  $\Upsilon(T)$ , photoionization cross sections  $\sigma_{PI}$ , recombination rate coefficients  $\alpha_R(T)$ , and  $f$ -values.

### 3.1. Electron Impact Excitation

One main aim of the IP is to compute collisional data for the iron-peak elements in various ionization stages. Collision strengths and rates for electron impact excitation (EIE) of all iron ions, Fe I - Fe XXVI, and other ions have been obtained. For example, Fe XVII, important in EUV and X-ray astronomy, has been recently studied with a large-scale BPRM calculation (Chen & Pradhan 2002) using a 89-level wavefunction expansion including up to  $n = 4$  levels. Their results show extensive resonance structures in the collision strengths that considerably enhance the rate coefficients (Fig. 1a). The corresponding line ratios are in good agreement with observations (Fig. 1b); filled squares are

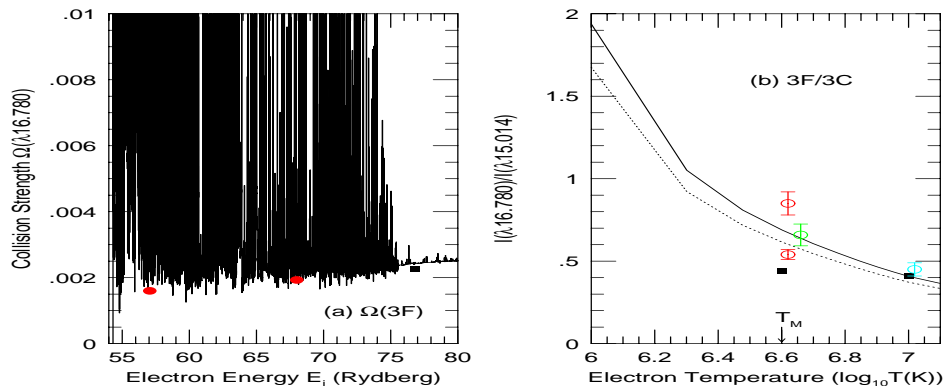


Figure 1. (a) BPRM collision strength  $\Omega$  for the forbidden 3F line; filled circles and square are non-resonant distorted wave calculations; (b): forbidden to resonance line ratio 3F/3C vs. T from a 89-level C-R model. The electron densities for solid-line and dot-line curves are  $10^{13}$  and  $10^9$   $\text{cm}^{-3}$  respectively. The 4 open circles with error bars are observed and experimental values; filled squares are values using distorted wave cross sections.

ratios obtained using previous cross sections that differ from observations at low temperatures. This is of considerable importance in photoionized x-ray plasmas that have temperatures of maximum abundance much lower than that in coronal equilibrium  $T_m \sim 4 \times 10^6$  K for Fe XVII, as marked.

Reviews and extensive compilations of available theoretical data sources for EIE collision strengths can be found in Pradhan & Gallagher (1992), Pradhan & Peng (1995) and Pradhan & Zhang (2001). A table of recommended data for effective collision strengths and A-values for ions from these references is available on-line from [www.astronomy.ohio-state.edu/~pradhan](http://www.astronomy.ohio-state.edu/~pradhan)

### 3.2. Photoionization and Recombination

The CC approximation, utilising the powerful R-matrix method, yields in an ab initio manner: (A) self-consistent photoionization and recombination cross sections using identical wavefunction expansions for both processes over all energies, (B) unified e-ion recombination (RR and DR) rates at all temperatures of interest, and (C) level-specific recombination rates for a large number of atomic levels. In contrast to simple approximations that artificially treat RR and DR separately, with different methods and over limited energy and temperature ranges, the present method accounts for e-ion recombination as it occurs in nature.

*Photoionization* The CC approximation enables the calculation of photoionization cross sections  $\sigma_{PI}$  for the ground and large number of excited bound states; both OP and IP typically consider all states up to  $n \leq 10$ . The cross sections include delineated autoionizing resonances upto  $\nu \leq 10$ , for each Rydberg

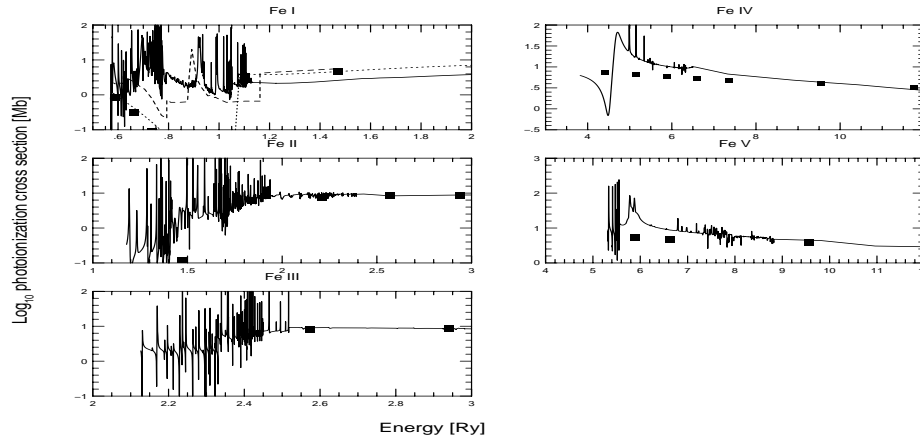


Figure 2. Photoionization cross sections,  $\sigma_{PI}$ , of the ground state of Fe I - Fe V, show large enhancements (the Y-axis is on a Log-scale) compared with previous works without resonances (e.g. Reilman and Manson 1979, filled squares; and Verner et al 1993).

series belonging to the various core thresholds. The resonances can enhance the background cross sections considerably. Fig. 2 shows the ground state photoionization cross sections of Fe I to Fe V (Bautista, Nahar, & Pradhan 1994-1997) dominated by extensive resonances. The enhancement in the background is up to three orders of magnitude for Fe I, over an order of magnitude for Fe II, and  $\sim 50\%$  for Fe III.

Channel couplings show important features that are nonexistent in simpler (e.g. central-field or screened-hydrogenic) approximations. One important feature is the photo-excitation-of-core (PEC) resonances in the excited state  $\sigma_{PI}$ . Fig. 3 shows  $\sigma_{PI}$  of excited series of states,  $3d^5ns(^7S)$  with  $5 \leq n \leq 11$ , of Fe III. The background cross section falls monotonically for each state until  $\sim 1.73$  Ry, where a strong and wide PEC resonance (pointed by the arrow) enhances the background considerably. The energy corresponds to the excited core threshold  $3d^44p(^6P^o)$  state of Fe IV. The photon at this energy is absorbed by the core in the dipole allowed transition from the ground state  $3d^5(^6S) \rightarrow 3d^44p(^6P^o)$ , while the valence electron remains a ‘spectator’. The electron is ejected when the core drops to ground state (PEC is the inverse process of DR). This enhancement contradicts the usual assumption of hydrogenic behavior of excited states, and can affect both the photoionization and recombination rates at high temperatures.

All  $\sigma_{PI}$  obtained under the OP, and for some complex ions,  $LS$  coupling approximation has been employed. However, relativistic BPRM approximation is now implemented for highly charged ions, such as Fe XXIV, Fe XXV, C IV, C V (Nahar, Pradhan, Zhang 2000, 2001) etc. Some large atomic systems, such as Fe XVII (Zhang, Nahar & Pradhan 2001), are under investigation including relativistic fine structure.

*Electron-ion Recombination* Fig. 4 presents the total unified recombination rate coefficient  $\alpha_R(T)$  for iron ions, Fe I - Fe V (solid, Nahar, Bautista, & Prad-

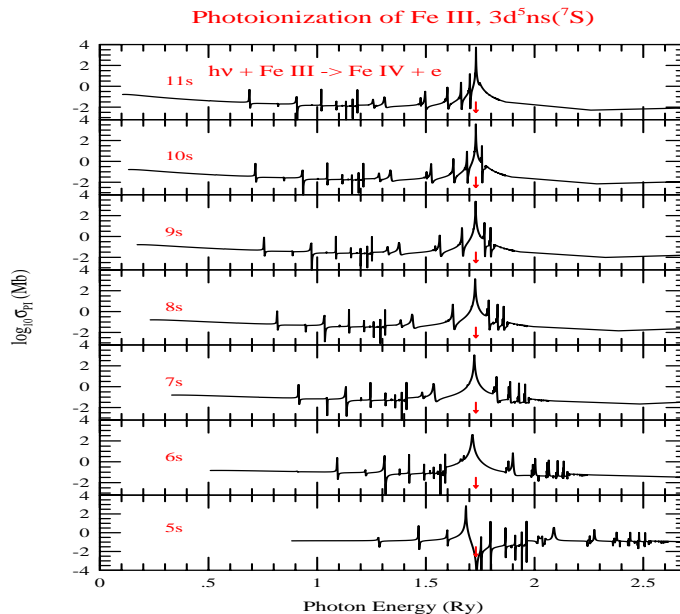


Figure 3. Photoionization cross sections,  $\sigma_{PI}$ , of the excited states of states,  $3d^5np(^7P^o)$ , of Fe III illustrating large PEC resonance.

han 1996-1999). The general features of the unified rate over a wide temperature ( $T$ ) range are as follows: At very low  $T$ , when electrons are not energetic enough to form doubly excited autoionizing states, recombination is dominated by RR. The rate decreases with  $T$  until, at high  $T$ , when it rises again due to dominance by DR. Comparison of the unified rates with the *sum* of the earlier RR rates from central field calculations, and the high temperature DR rates mainly from the Burgess general formula, show either an underestimate or overestimate by several factors at temperatures of maximum abundance of Fe I - V (dashed lines in lower panels in Fig. 4). The large differences between the unified rate and the sum of the earlier (RR+DR) results illustrates the fundamental inaccuracy of separate treatments of RR and DR. Resonances are inextricably related to the coupling within the wavefunction expansion, and may not be separated from the non-resonant background, as seen in the photoionization cross sections in Fig. 3. The inclusion of this quantum mechanical interference in the R-matrix method is the basic advance enabled by the unified method.

Recently Gorczyca et.al. (2002) discuss certain effects of marginal importance, such as radiation damping of some resonances, radiative decay between autoionizing states, and forbidden transitions in the core (DR is dominated by dipole allowed transitions). They selectively consider small energy ranges, and/or a few resonances, in one or two highly charged ions where a separation between RR and DR may not be too inaccurate. Although Gorczyca et. al. describe the neglect of these effects as 'shortcomings of the R-matrix method', the overall effect on total recombination rates of practical astrophysical importance does not exceed about 10% - well within the accuracy of the R-matrix method -



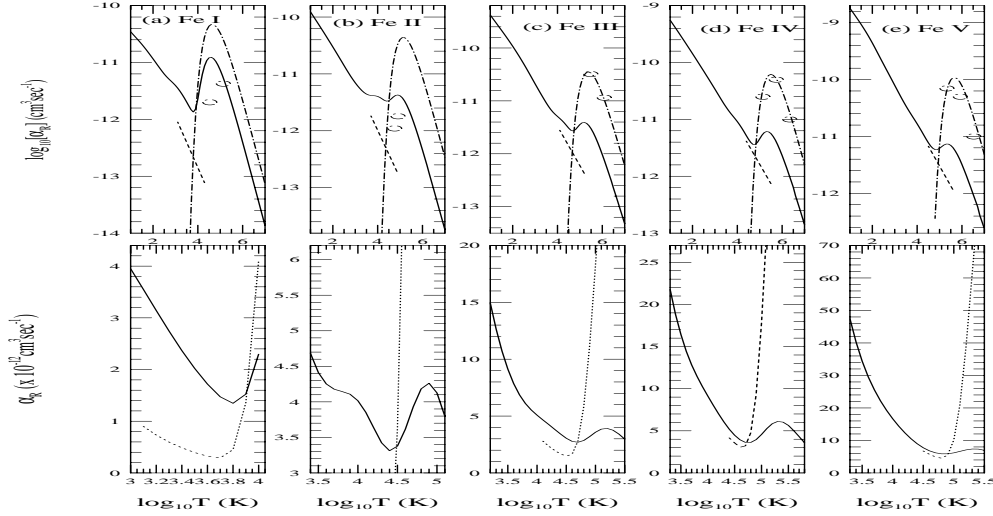


Figure 4. Unified total recombination rate coefficients ( $\alpha_R(T)$ ) (solid), compared with the previous RR and DR calculations, in upper panels. Comparison with the sum of RR+DR rates computed separately in previous works is shown in lower panels on an expanded scale close to temperatures of maximum ionic abundance; For example, the unified rate for Fe I is higher than previous (RR+DR) rates by up to a factor of 4 for  $T < 10^4$  K.

even for their example of Fe XVIII. In any event, these effects (particularly radiation damping) are, or may be, considered in our formulation if necessary. We note that other effects, such as external field ionization of high- $n$  Rydberg levels, are likely to be much more important. We emphasize that the unified R-matrix method is the only method generally capable of computing unified recombination rates, and consistent with scattering and photoionization calculations, for all atomic systems.

The unified rates are valid over a wide range of temperatures for all practical purposes, in contrast to RR and DR rates obtained using different approximations in different temperature ranges. Following is the list of over 45 atoms and ions for which self-consistent sets of  $\sigma_{PI}$  and  $\alpha_R(T)$  have so far been obtained (reported in Nahar and Pradhan 1997, and subsequent publications in ApJS, and in others and on [www.astronomy.ohio-state.edu/~pradhan](http://www.astronomy.ohio-state.edu/~pradhan)):

Carbon: C I, C II, C III, C IV, C V, C VI

Nitrogen: N I, N II, N III, N IV, N V, N VI, N VII

Oxygen: O I, O II, O III, O IV, O V, O VI, O VII, O VIII

Silicon: Si I, Si II, Si III, Si IV, Si V, Si VI

Sulfur: S I, S II, S III, S IV, S V, S VI, S VII, S VIII, S IX, S X, S XI

Iron: Fe I, Fe II, Fe III, Fe IV, Fe V, Fe VI, Fe VII, Fe VIII, Fe IX, Fe X, Fe XI, Fe XII, Fe XIII, Fe XIV, Fe XV, Fe XVI, Fe XVII, Fe XVIII, Fe XIX, Fe XX, Fe XXI, Fe XXII, Fe XXIII, Fe XXIV, Fe XXV, Fe XXVI

C-like: F IV, Ne V, Na VI, Mg VII, Al VIII, Ar XIII, Ca XV

Other ions: Ar V, Ca VII, Ni II

The complete data include state specific photoionization cross sections and recombination rates for hundreds of bound levels with  $n \leq 10$  for each ion.

### 3.3. Transition probabilities of atoms and ions

Under the IP transition probabilities are evaluated in the BPRM approximation including relativistic fine structure, in contrast OP work for dipole allowed  $LS$  multiplets. Both the dipole allowed and spin-forbidden E1 intercombination transitions are obtained. Owing to fine structure, the sets of data for  $f$ - and  $A$ -values are considerably larger. For example, the large scale calculations for Fe V transition probabilities resulted in about  $1.5 \times 10^6$  transitions among 3865 fine structure levels (Nahar et al. 2000).

The forbidden electric quadrupole (E2) and octupole (E3), magnetic dipole (M1) and quadrupole (M2), transitions are also being evaluated in atomic structure calculations using SUPERSTRUCTURE (Eissner et al. 1974) and other codes.

The BPRM fine structure energy levels are analysed using quantum defects and channel weights to obtain complete spectroscopic identifications,  $(C_t S_t L_t J_t \pi_t n \ell) SLJ \pi$  where  $(C_t S_t L_t J_t \pi_t)$  denotes the N-electron core configuration  $C_t$ , spin and orbital angular momenta  $S_t L_t$ , and parity  $\pi_t$ ;  $n \ell$  the outer or valence electron,  $SL$  are the total spin and orbital angular momenta, and  $J \pi$  are the total angular momentum and parity of the (N+1)-electron system.

Accurate fine structure transition probabilities have been obtained for a number of ions including:

Fe ions: Fe V, Fe XVII, Fe XXI, Fe XXIII, Fe XXIV, Fe XXV

Li-like: C IV, N V, O VI, F VII, Ne VIII, Na IX, Mg X, Al XI, Si XII, S XIV, Ar XVI, Ca XVIII, Ti XX, Cr XXII, Ni XXVI

He-like: C IV, N V, O VI, F VII, Ne VIII, Na IX, Mg X, Al XI, Si XII, S XIV, Ar XVI, Ca XVIII, Ti XX, Cr XXII, Ni XXVI

Other ions: C II, C III, O IV, S II, Ar XIII, Na III, Cl-like ions

The latest BPRM work on transition probabilities of Fe XVII has resulted in  $2.6 \times 10^4$  dipole allowed and intercombination E1 transitions. They correspond to 490 fine structure levels of  $1/2 \leq J \leq 17/2$  of even and odd parities with  $n \leq 10$  &  $0 \leq l \leq 9$ ,  $0 \leq L \leq 8$ , and core  $2s^2 2p(^2P_{3/2,1/2}^o)$ ,  $2s 2p^6(^2S_{1/2})$ . Oscillator strengths for about 360 electric quadrupole and magnetic dipole and a large number of E3 and M2 transitions have also been obtained. A sample table of transitions in Fe XVII with spectroscopic identifications is presented in Table I.

### 3.4. Ionization structure of a planetary nebula

Fig. 5 shows the ionization structure of Fe ions in a planetary nebula under typical conditions: Solid curves are ionic fractions from new cross sections and recombination rates; the dotted and dashed curves are from previous data. A large discrepancy is found for Fe V and Fe VI ionic fractions, by a factor of two at  $T_{eff} = 100,000$  K.

Table I: Transition probabilities of Fe XVII.  $g=2J+1$ .

$C_i$	$C_j$	$T_i$	$T_j$	$g_i$	$g_j$	$E_{ij}$ (Å)	$f$	$A$ ( $s^{-1}$ )
$2s22p6$	$-2s22p53s$	$^1S^e$	$^3P^o$	1	3	17.1	1.223E-01	9.35E+11
$2s22p6$	$-2s22p53s$	$^1S^e$	$^1P^o$	1	3	16.8	1.008E-01	7.96E+11
$2s22p6$	$-2s22p54s$	$^1S^e$	$^3P^o$	1: 1	3: 8	12.7	2.286E-02	3.16E+11
$2s22p6$	$-2s22p54s$	$^1S^e$	$^1P^o$	1: 1	3: 9	12.5	1.758E-02	2.49E+11
$2s22p6$	$-2s22p55s$	$^1S^e$	$^3P^o$	1: 1	3:13	11.4	1.003E-02	1.71E+11
$2s22p6$	$-2s22p55s$	$^1S^e$	$^1P^o$	1: 1	3:14	11.3	1.219E-02	2.13E+11
$2s22p6$	$-2s22p53d$	$^1S^e$	$^3P^o$	1	3	15.4	8.136E-03	7.58E+10
$2s22p6$	$-2s22p53d$	$^1S^e$	$^3D^o$	1	3	15.3	6.208E-01	5.93E+12
$2s22p6$	$-2s22p53d$	$^1S^e$	$^1P^o$	1	3	15.0	2.314E+00	2.28E+13
$2s22p6$	$-2s22p54d$	$^1S^e$	$^3P^o$	1: 1	3:10	12.3	3.281E-03	4.81E+10
$2s22p6$	$-2s22p54d$	$^1S^e$	$^3D^o$	1: 1	3:11	12.3	3.594E-01	5.31E+12
$2s22p6$	$-2s22p54d$	$^1S^e$	$^1P^o$	1: 1	3:12	12.1	3.987E-01	6.03E+12
$2s22p6$	$-2s2p63p$	$^1S^e$	$^3P^o$	1: 1	3: 6	13.9	3.501E-02	4.03E+11
$2s22p6$	$-2s2p63p$	$^1S^e$	$^1P^o$	1: 1	3: 7	13.8	2.835E-01	3.30E+12
$2s22p6$	$-2s2p64p$	$^1S^e$	$^3P^o$	1: 1	3:18	11.0	1.073E-02	1.96E+11
$2s22p6$	$-2s2p64p$	$^1S^e$	$^1P^o$	1: 1	3:19	11.0	9.190E-02	1.68E+12
$2s22p53s$	$-2s22p53p$	$^3P^o$	$^3P^e$	3	1	296.0	3.354E-02	7.66E+09
$2s22p53s$	$-2s22p53p$	$^3P^o$	$^3P^e$	3	3	262.7	5.893E-05	5.70E+06
$2s22p53s$	$-2s22p53p$	$^3P^o$	$^3P^e$	5	3	252.5	4.985E-03	8.69E+08
$2s22p53s$	$-2s22p53p$	$^3P^o$	$^3P^e$	3	5	340.4	9.075E-02	3.13E+09
$2s22p53s$	$-2s22p53p$	$^3P^o$	$^3P^e$	5	5	323.5	6.913E-02	4.41E+09
$LS$		$^3P^o$	$^3P^e$	9	9		8.959E-02	6.71E+09
$2s22p63s$	$-2s22p53p$	$^1P^o$	$^3P^e$	3	1	413.8	9.557E-03	1.12E+09
$2s22p63s$	$-2s22p53p$	$^1P^o$	$^3P^e$	3	3	351.6	4.162E-02	2.25E+09
$2s22p63s$	$-2s22p53p$	$^1P^o$	$^3P^e$	3	5	506.3	1.464E-03	2.29E+07

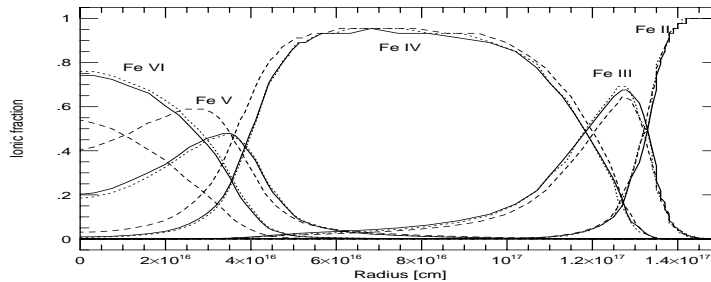


Figure 5. Ionization fractions of Fe ions in a typical planetary nebula obtained using the new data (solid), compared with those obtained using previous calculations.

#### 4. TIPTOPBASE: atomic radiative and collisional data

The current number of the series publication is 51. The IP website address is [http : //www.usm.uni - muenchen.de/people/ip/iron - project.html](http://www.usm.uni-muenchen.de/people/ip/iron-project.html). The IP and related works can also be found at [http : //www.astronomy.ohio - state.edu/ ~pradhan](http://www.astronomy.ohio-state.edu/~pradhan). The extensive amount of atomic data and opacities obtained under the OP and the IP are available electronically through the existing database, TOPbase and through its planned extension TIPTOPBASE (C. Mendoza and the OP/IP team).

The radiative atomic and opacity data obtained under the OP are accessible via TOPbase from two websites: ([http : //heasarc.gsfc.nasa.gov](http://heasarc.gsfc.nasa.gov) at Goddard, NASA and [http : //vizier.u - strasbg.fr/OP.html](http://vizier.u-strasbg.fr/OP.html) at CDS). TOPbase data, for ions with  $Z = 1 - 14, 16, 18, 20, 26$ , are:

- (i) Photoionization cross sections of bound  $LS$  terms,
- (ii) Transition probabilities and  $f$ -values,
- (ii) Energy levels, EQN ( $\nu$ ), radiative lifetimes,
- (iv) Monochromatic and Rosseland mean opacities

The new database, TIPTOPbase (under development, C. Mendoza & the OP/IP team) will have collisional as well as radiative data, including

- (i) All radiative data from TOPbase
- (ii) Electron impact excitation collision strengths and rate coefficients for all iron ions, Fe I - Fe XXVI, Ni III, and other ions,
- (iii)  $A$ -values for transitions in the target ion
- (iv) Inner-shell photoionization ("tail") cross sections
- (v) Radiative data for new elements through all ionization stages: P, Cl, K, and Ni II, Ni III,
- (vi) More extended set of radiative data from repeated CC calculations

- (vii) Radiative data ( $\sigma_{PI}$  and  $f$ -values) for fine structure levels including relativistic effects
- (viii) Total and level specific unified (RR+DR) recombination rate coefficients
- (ix) Inner-shell radiative data for Fe ions - "PLUS" data
- (x) On-line computational of opacities and radiative accelerations for user-specified mixtures of elements ("customized" opacities and radiative forces).

#### 4.1. TIPTOPbase: On-line computation

Seaton has developed efficient codes for on-line computation of 'customized' mixture opacities and radiative accelerations ('levitation') in stars.

i) Stellar opacities, Radiative forces: On-line interactive facility to compute mean and monochromatic opacities, and radiative forces, as function of temperature, density, and user-specified mixture of elements.

1) Monochromatic opacities  $\kappa_\nu$  for 17 elements: H, He, C, N, O, Ne, Na, Mg, Al, Si, S, Ar, Ca, Cr, Mn, Fe and Ni (Seaton et al 1994) as function of  $\log(u = h\nu/kT)$  at a mesh of  $(T, N_e)$  are tabulated.

(2) Tables of Rosseland mean  $\kappa_R(T, \rho)$ , with standard solar and non-solar, abundances where  $\rho$  is the mass density (g/cc).

$$\frac{1}{\kappa_R} = \frac{\int_0^\infty \frac{1}{\kappa_\nu} g(u) du}{\int_0^\infty g(u) du}, \quad g(u) = \frac{15}{4\pi^4} u^4 e^{-u} (1 - e^{-u})^{-2},$$

where  $g(u)$  is the Planck weighting function have been calculated for different chemical compositions H (X), He (Y) and metals (Z), such that  $X+Y+Z = 1$ .

Partial derivatives of Rosseland means,  $\left(\frac{\partial \log(\kappa_R)}{\partial \log(T)}\right)_\rho, \left(\frac{\partial \log(\kappa_R)}{\partial \log(\rho)}\right)_T$ , required for stellar structure and pulsation studies are also calculated.

ii) Radiative accelerations:

Radiative acceleration,  $g_{rad}(k)$  for an element  $k$  is (Seaton 1997),

$$g_{rad}(k) = (1/c) \int \sigma_\nu(k) F_\nu d\nu / M(k),$$

where  $M(k)$  is the mass of atom  $k$  and the flux  $F = \int F_\nu d\nu$  is related to the Rosseland mean  $\kappa_R$  as  $F_\nu = (\frac{\kappa_R}{\kappa_\nu})(h/kT)g(u)$ .

Radiative diffusion can lead to large changes in abundances of individual elements in a star as gravitational forces are counteracted by radiative levitation. For diffusion, one requires  $g_{rad}(k)$  for all depths in the star, as a function of the abundance of element  $k$ . Interpolation codes will be provided in TIPTOPbase to obtain radiative accelerations for user-specified mixture and mesh of temperature and density.

## 5. Conclusion

The current status of large-scale ab initio close coupling R-matrix calculations for radiative and collisional processes is reported. The Iron Project Breit Pauli R-matrix radiative calculations include large numbers of dipole allowed and inter-combination transitions. Self-consistent sets of atomic data for photoionization

and unified (electron-ion) recombination (including RR and DR) are obtained, and should yield more accurate photoionization models. Work is in progress for heavy ions of the iron group elements.

**Acknowledgments.** Partial supports by the U.S. National Science Foundation and NASA are acknowledged.

## References

- Bautista, M.A. 1996, A&AS 119, 105, *ibid* 1997, A&A 122, 167; Bautista M.A. & Pradhan, A.K. 1997, A&AS 126, 365; Nahar, S.N. & Pradhan, A.K. 1994, J. Phys. B 27, 429; Nahar, S.N. 1996, Phys. Rev. A 53, 1545 ( $\sigma_{PI}$  for Fe ions)
- Bell, R.H. & Seaton, M.J. 1985, J. Phys. B, 18, 1589
- Berrington, K.A., Burke, P.G., Butler, K., Seaton, M.J., Storey, P.J., Taylor, K.T., & Yu, Yan, 1987, J.Phys. B, 20, 6379; Berrington, K.A., Eissner, W.B., & Norrington, P.H. 1995, CPC, 92, 290; Burke, P.G. & Robb, W.D. 1975, Adv. At. Mol. Phys., 11, 143
- Chen, G.X. & Pradhan, A.K. 2002, Phys.Rev.Lett, 89, 013202-1
- Eissner, W., Jones, S. W., & Nussbaumer, N. 1974, CPC, 8, 270
- Gorczyca, T.W., Badnell, N.R., & Savin, D.W. 2002, Phys. Rev. A 65, 062707
- Hummer, D.G., Berrington, K.A., Eissner, W., Pradhan, A.K., Saraph, H.E., & Tully, J.A. 1993, A&A, 279, 298
- Nahar, S.N. & Pradhan, A.K. 1994, Phys. Rev. A, 49, 1816; 1995, ApJ, 447, 966
- Nahar, S.N. 1996, Phys. Rev. A 53, 2417; *ibid* 1997, Phys. Rev. A 55, 1980, Nahar, S.N. & Bautista, M.A. 1999, ApJS120, 327; Nahar, S.N., Bautista, M.A., & Pradhan, A.K. 1997, ApJ479, 497; *ibid* 1998, Phys. Rev. A 58, 4593 ( $\alpha_R$  for Fe ions)
- Nahar S.N., Delahaye F., Pradhan A.K., & Zieppen C.J. 2000, A&AS144, 141
- Nahar, S.N., & Pradhan, A.K. 1997, ApJS, 111, 339
- Nahar, S.N., Pradhan, A.K., & Zhang, H.L. 2000, ApJS131, 375, *ibid* 2001, ApJS133, 255; Zhnag, H.L., Nahar, S.N., & Pradhan, H.L. 2001, Phys. Rev. A 64, 032719
- Pradhan, A.K. & Gallagher, J.W. 1992, At. Data and Nucl. Data Tables, 52, 227; Pradhan, A.K. & Peng, J. 1995, in Proceedings of the Space Telescope Science Institute Symposium on *Analysis of Emission Lines*, pp 8-34, (in honor of the 70th birthdays of D.E. Osterbrock & M.J. Seaton). Ed: R.E. Williams and M. Livio, Cambridge University Press (1995); Pradhan, A.K., & Zhang, H.L. 2001, *Electron Collisions with Atomic Ions*, in Landolt-Börnstein Volume 17 *Photon and Electron Interactions with Atoms, Molecules, Ions*, Springer-Verlag (2001), I.17.B, pp 1-102 (Ed: Y. Itikawa).
- Seaton, M.J. 1987, J.Phys.B, 20, 6363
- Seaton, M.J., Yu, Y., Mihalas, D., Pradhan, A.K. 1994, MNRAS 266. 805

*The Opacity Project 1 and 2*, compiled by the Opacity Project team (Institute of Physices, London, UK, 1995, 1996)